Hindawi
Shock and Vibration
Volume 2020, Article ID 8814009, 12 pages
https://doi.org/10.1155/2020/8814009

Research Article

Dynamic Response Characteristics of the Structures under Excavation by High-Efficiency Blasting in the Urban Ultradeep Foundation Pit

Zhen Lei,[1] **Qing Chen**,[2] **Wen Zhao**,[3] **Yu-Jing Li**,[3] **and Zheng-Hua Gao**[4]

[1]*Mining College, Guizhou Institute of Technology, Guiyang 550025, China*
[2]*Public Security Corps of Guizhou Provincial Public Security Department, Guiyang 550001, China*
[3]*Guizhou Kaiyuan Blasting Engineering Co., Ltd., Guiyang 551400, China*
[4]*Department of Mechanics and Civil Engineering, China University of Mining and Technology, Beijing 100083, China*

Correspondence should be addressed to Zheng-Hua Gao; 837224105@qq.com

Received 3 July 2020; Revised 23 October 2020; Accepted 29 November 2020; Published 9 December 2020

Academic Editor: M. Z. Naser

Copyright © 2020 Zhen Lei et al. This is an open access article distributed under the Creative Commons Attribution License, which permits unrestricted use, distribution, and reproduction in any medium, provided the original work is properly cited.

To ensure the safe and efficient excavation of ultradeep foundation pits in a complex urban environment, the ultradeep foundation pit excavation project of Liuguangmen Urban Complex in Guiyang City was taken as the study point. A high-efficiency blasting method was proposed for the excavation of vibration-isolating slot and electronic detonators, and a three-dimensional spatial calculation model of the foundation pit structure was established. In addition, the field test and numerical simulation of the blasting vibration were developed. The feasibility of the high-efficiency blasting method was demonstrated, and the propagation law of the dynamic response characteristic parameters of the structure was explored using an electronic detonator and vibration-isolating slot. The results show that the electronic detonator carried out peak shaving within the group, unloading waves between the groups, and the blocking effect of the vibration-isolating slot, and all these effectively reduced the peak stress and peak particle vibration velocity, evenly distributed the vibration velocity, and guaranteed the safety of the surrounding existing buildings, proving the feasibility of the efficient blasting method. There is a "wall effect" at the supporting pile, whose propagation velocity is lower than that inside the rock mass, and the PPV is radial X > tangential Y > vertical Z. The peak values of stress, strain, and PPV all decrease with increasing supporting pile height, and there is an inflection point at 20 m. The internal nodes of the pile reciprocate without sharp change and failure in displacement. The peak displacement of different nodes is in the order $X > Y > Z$ with increasing pile height, and the maximum peak value is 0.08 mm.

1. Introduction

The safe and efficient excavation of foundation pits in a complex urban environment has been investigated in detail. For example, Li et al. [1] adopted a vibration-isolating hole combined with long and short time delays of an electronic detonator on the basis of controlled dosage to solve the problem of excavation of large quantity and deep rock foundation pit with complex strata in downtown area. Gao et al. [2] analyzed the dynamic response law and vibration velocity safety threshold of an adjacent sewage pipeline under the blasting action of foundation pit excavation. Ma et al. [3] carried out a shaking table model test to study the seismic stability of the retaining structure of underground continuous wall during the construction of deep foundation pit. Zhang et al. [4] studied the effect of different traffic load coefficients and supporting structure parameters on the stability of the supporting structure of deep foundation pit under construction. Xue et al. [5] discussed the vibration response of train load to the retaining structure of foundation pit and proposed the measures of velocity limit and vibration reduction. Xie et al. [6] conducted vibrational, acoustic, and numerical simulation tests on the vibration velocity threshold of foundation pit blasting. Dowding et al. [7] studied the strain response characteristics of the urban structure under blasting excavation. Yankelevsky et al. [8]

studied the blasting resistance and response of reinforced concrete building structures under the terrorist threats of blasting in Israeli urban areas. Meins et al. [9] summarized the structural response of high-rise buildings under short-distance blasting in New York City, providing a reference model for the development of the standard for short-distance blasting in high-rise buildings. Xie et al. [10] optimized the shallow-buried tunnel blasting scheme based on the complex urban environment and controlled the vibration velocity below 1.5 cm/s. Wang et al. [11] investigated ways to reduce vibration and monitor the foundation pit blasting to protect surrounding buildings. Zhou et al. [12] studied the dynamic response, damage evolution, and failure forms of BFRP bars in shallow-buried urban tunnels under repeated explosions. Zhang et al. [13] analyzed the spatial distribution characteristics of blasting vibration velocity and dynamic stress of high-rise buildings through dynamic numerical analysis. Wang et al. [14] captured the acceleration spectrum of Wenchuan earthquake to establish a reasonable three-dimensional seismic response model, simulating the dynamic stability, instability abrupt transition process, and time effect characteristics of the foundation pit and support structure under strong earthquake. Wei et al. [15] simulated the vibration velocity response of different structures by the dynamic analysis method and verified that the vibration-isolating slot is an effective damping method. Sun et al. [16] experimentally investigated the damping effect of the vibration damping holes in the foundation pit, analyzed the vibration velocity attenuation law and the vibration-damping rate of the single- and double-row vibration-damping holes, and calculated and verified them by numerical simulation. However, there are a few reports on the evolution law of the dynamic response characteristic parameters under high-efficiency blasting effect of excavation vibration-isolating slot and electronic detonator initiation.

In view of this, based on the excavation of ultradeep foundation pits (the excavation depth exceeds 15 m) in the complicated environment around Liuguangmen in Guiyang city, combined with the vibration reduction excavation technology of electronic detonator blasting and the characteristics of the vibration-isolating slot, in this study, a high-efficiency blasting excavation and slope support scheme for foundation pits and blasting vibration monitoring scheme were formulated. A digital network vibration meter (CBSD-VM-M01) was used to conduct on-site blasting vibration test and analyze the vibration response characteristics of existing buildings according to the test results. Then, based on the actual blasting site, a three-dimensional spatial calculation model of the foundation pit structure was established to study the dynamic response law of the supporting structure under the blasting excavation of the ultradeep foundation pit.

2. Experimental Design and System

2.1. Test Site. The experimental site is the foundation of an urban complex engineering foundation pit, located in the political and cultural center of Guiyang city, close to the provincial government building. The width of the foundation pit is about 120 m, the maximum section length is more than 260 m, and the maximum excavation depth is up to 42 m. The underground part of the proposed building consists of two floors of sewage treatment structure, three floors of the underground parking lot, and one floor of commercial district from bottom to top. Figure 1 shows the complex surrounding environment of the foundation pit excavation. Buildings (structures) close to the foundation pit include residential buildings at 22 m in the north, light rail stations under construction at 20 m in the west, and specialized hospitals at 55 m.

2.2. Blasting Excavation Scheme. The upper layer of the rock mass is weathered, while the lower layer is relatively hard, and fissure karst is developed. Blasting was used to break the rock in the area where conditions permit. The slope of the foundation pit is vertical, and an anchor cable row pile with a diameter of 1800 mm and a pile center distance of 1500 mm apart was used for support. Part of the adjacent pile rock mass was retained during the earth-rock excavation. After the pile body reaches the design strength and the anchor cable is gradually applied to prestress, the retained rock mass was broken and cleared mechanically.

In terms of the adverse effects of blasting of this project, vibration, the main control object, was mainly controlled by the single-hole charge, the initiation network, and the vibration propagation path. According to Sadov's empirical formula for vibration calculation [17] and similar construction experience, the blasting area and the mechanical broken area (rock mass within 15 m of the adjacent pile) are divided and the single-hole charge is strictly controlled. Table 1 shows the hole pattern parameters of the blasting area.

The effect of the Wenchuan earthquake acceleration on steel-supported foundation pit was studied following literature procedure [18]. The instability process is divided into three stages: reciprocating motion and a sharp increase in displacement and instability with the corresponding periods of $t \leq 10$ s, $10 \leq t \leq 20$ s, and $t \geq 20$ s, respectively. The design of the detonation network ensures that the blasting time of the hole is independent of each other, avoids vibration superposition, and controls the single duration of vibration. Based on the convenience of digital electronic detonator delay setting, the detonation network of the electronic detonator was designed to have a long and short delay, namely, the blastholes in the network are grouped (one group has 5-6 holes), the holes were set as short delay (45 ms) within the group and long delay (1500 ms) between the groups. The delay network is shown in Figure 2. A vibration-isolating slot is a shallow ditch dug in the vicinity of buildings and other facilities to prevent vibration harm. To ensure the safety of the surrounding structures, the slot was set with a depth of 4 m, a width at the top of 4 m, and a width at the bottom of 3 m.

2.3. Blasting Vibration Monitoring Design and Experimental System

2.3.1. Monitoring Design. A huge amount of energy is released instantly in the process of blasting as a result of

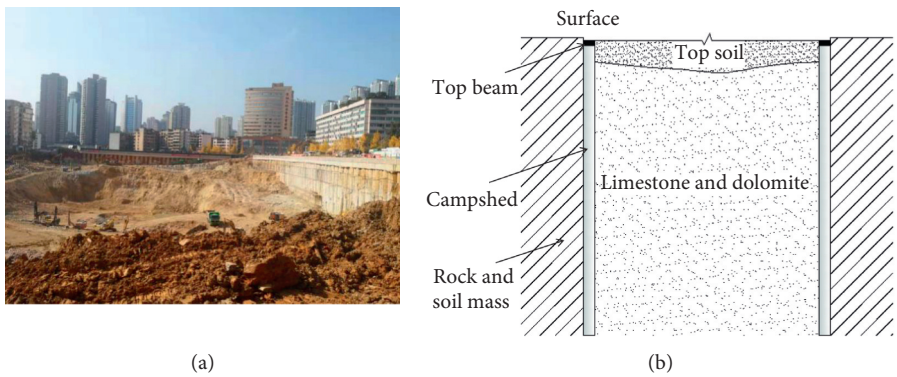

Figure 1: Surrounding environment of the experimental site: (a) the real picture and (b) the profile picture.

Table 1: Parameters for blasting.

Position		Bench height (m)	Hole spacing (m)	Row spacing (m)	Overdrilling depth (m)	Borehole diameter (mm)	Length of stemming (m)	Single-hole charge (kg)
Distance from supporting pile	>20 m	4.0	3.0	2.5	0.5	90	2.9	8
	15–20 m	3.5	3.0	2.5	0.5	90	2.8	6

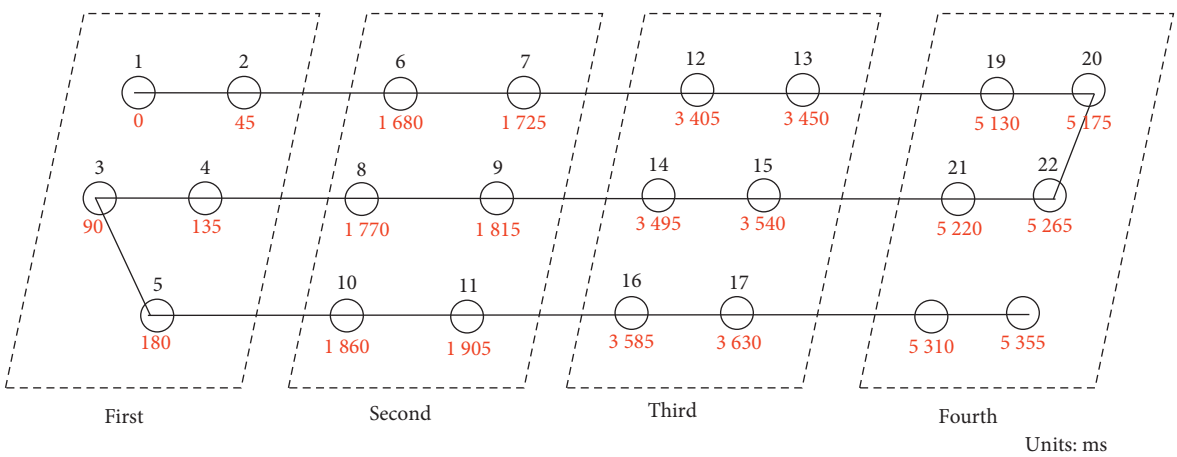

Figure 2: Time-delayed blasting of the electronic detonator network.

the detonation of the explosive. A part of this energy is used for the crushing of the mining rock and the compaction of the soil, rock, and mud, while the other part is absorbed by the surrounding rock or soil rock and mud. In addition, the released energy spreads in all the directions in the form of an elastic vibration wave, causing vibration in the adjacent supporting structure and the existing building particles. To reveal the vibration response characteristics of the structure, a digital network vibration meter (CBSD-VM-M01) was used for the field test. A total of two vibration monitoring points were arranged, in which the measuring points 1 and 2 were arranged in the existing residence and the support structure, respectively, as shown in Figure 3.

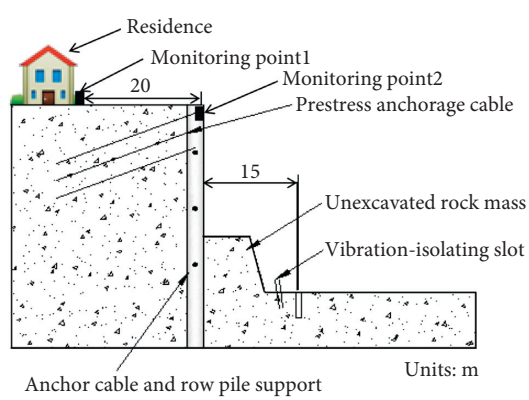

Figure 3: Schematic of the monitoring scheme.

According to the monitoring scheme, the dirt on the residential foundation surface and the supporting pile wall surface where the measuring point is located was cleaned. Then, adjust the X direction (radial direction) of the intelligent sensor of the vibration meter to keep consistent with the direction of the explosion source, connect the sensor with the surface of the ground (or support pile wall) with gypsum (or super glue and fixture), and make the instrument level center, while ensuring the fastness of connection. Finally, set the parameters of the vibration meter through the control analyzer and press "Collect" on the intelligent sensor to conduct the vibration data monitoring test.

2.3.2. Experimental System. Figure 4 shows the test system for the blasting vibration. The system mainly consists of a control analyzer, an intelligent sensor, a router, and a computer. When blasting was carried out, the intelligent sensor was fixed together with the existing building. The blasting action causes the surrounding building particles to vibrate, and the sensor housing vibrates accordingly. Under the action of inertia, the internal coil, damping ring, and core rod move relative to the housing, thus the coil generates induced electromotive force, which is converted into vibrational velocity. The control analyzer connects the intelligent sensor through the router to set vibration parameters and obtain vibration data and finally uploads the computer terminal for analysis and processing. According to the site environmental conditions and blasting vibration characteristics, the trigger level of the test device was set as 20%, the sampling frequency as 2 kHz, the recording duration as 6 s, and the delay as 0.2 s.

3. Analysis of Test Results of the Structural Vibration Response Characteristics

Figure 5 shows the characteristic curve of blasting vibration response of seismic wave extending to the existing buildings under the action of vibration-isolating slot and electronic detonator initiation. The vibration waveform of the first group (0–180 ms), the second group (1680–1905 ms), the third group (3405–3630 ms), and the fourth group (5130–5355 ms) was monitored during 0-1 s, 1.5–2.5 s, 3-4 s, and 5-6 s, respectively. In all the four groups, the PPV at the monitoring point of the existing houses was 0.210 cm/s, and the supporting pile was 0.195 cm/s. The duration of each group was roughly equal. The PPV and main frequency of each group are shown in Table 2.

Figure 5 shows the tested vibration waveform of the residence and the supporting pile, indicating that the stress transfer process caused by the blasting of the hole between groups is basically independent of each other. The vibrational velocity of each group was relatively uniform, the wave peak and trough of the vibration velocity between the groups were superimposed to reduce, and the staggering peak reduced the peak of the vibration velocity. There is a long time interval between the groups. After blasting the last hole of the previous group, the energy is not supplemented

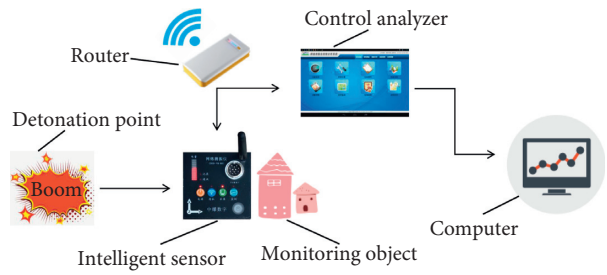

Figure 4: Blasting vibration testing system.

and the vibration velocity gradually decreases. In this way, the peak shaving within the group and unloading waves between the groups reduce the vibration.

Vibration is one of the adverse effects of blasting and is the main factor affecting the safety of construction and the most common cause of "disturbance in the surrounding structures and disturbing the people". Therefore, vibration must be checked and analyzed strictly. In Table 2 of the tested signal data, the PPV and main frequency of the residence and the supporting piles as a whole show the radial direction $X >$ tangential $Y >$ vertical Z with their PPV and main frequency corresponding to (0.210 cm/s, 21.27 Hz) and (0.195 cm/s, 18.35 Hz), respectively. Referring to relevant national regulations and studies on the vibration velocity threshold for disturbing residents [6], the threshold of this type of house was taken as 1.5 cm/s to minimize disturbance to the residents. The impact of this blasting stress disturbance on the residential building in this study met relevant regulations and is lower than the threshold of the nuisance security in relevant studies and regulations.

The PPV of radial, tangential, and vertical at the monitoring point (in the support pile) 15 m from the horizontal distance is 0.195, 0.148, and 0.029 cm/s, which are lower than that at the measuring point (in the residence), 35 m (0.210 cm/s in radial, 0.203 cm/s in tangential, and 0.041 cm/s in vertical), showing abnormalities. The reason is that the tested data of the residence are the internal propagation of the rock mass, while there is a wall surface between the supporting pile and the rock mass, resulting in the "wall effect," with propagation velocity lower than the internal velocity of the rock mass. In other words, the stress wave propagates, reflects, and stretches on the wall surface of the supporting pile, which leads to energy dissipation and thus reduces the propagation velocity.

4. Numerical Analysis of Dynamic Response Characteristics of the Structure

4.1. Numerical Calculation Model and Parameters

4.1.1. Calculation Model. The safety and stability of structure depend on its dynamic response under blasting disturbance. To explore the impact of the blasting process on the foundation pit support system and existing structures around it and prove the feasibility of the blasting scheme, the dynamic finite element software LS-DYNA was used to establish the numerical model of the lowest horizontal

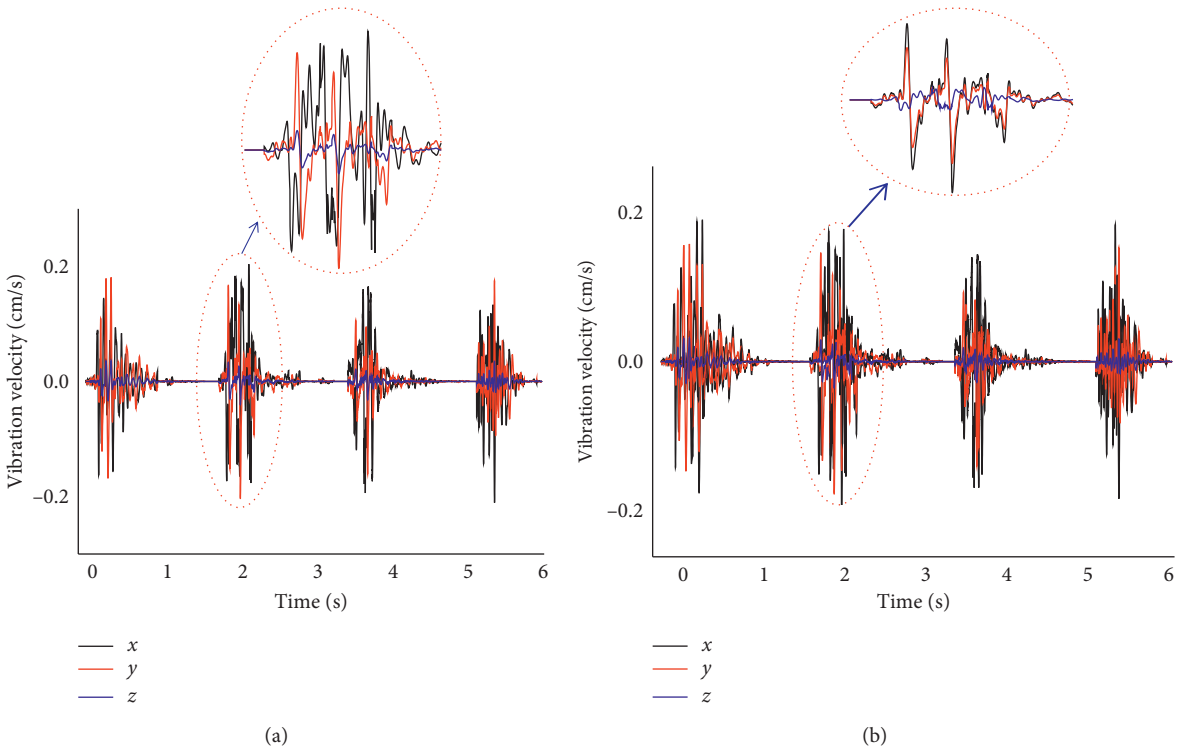

Figure 5: The characteristic curve of blasting vibration response of seismic wave: (a) the monitoring point in the residence and (b) the monitoring point in the supporting pile.

Table 2: The PPV and main frequency of the on-site monitored data.

Position	Distance (m)	Group number	Horizontal radial (*X*)		Horizontal tangential (*Y*)		Vertical (*Z*)	
			PPV (cm/s)	Main frequency (Hz)	PPV (cm/s)	Main frequency (Hz)	PPV (cm/s)	Main frequency (Hz)
Residence	35	1	0.169	21.27	0.182	13.69	0.033	10.63
		2	0.201		0.203		0.041	
		3	0.196		0.164		0.032	
		4	0.210		0.171		0.035	
Supporting pile	15	1	0.189	18.35	0.130	15.32	0.022	6.72
		2	0.195		0.148		0.028	
		3	0.170		0.116		0.027	
		4	0.186		0.126		0.029	

foundation pit blasting excavation. The fluid-solid coupling model was selected, and the Lagrange algorithm was used for rock and reinforced concrete. Considering that the material under the impact load of the explosion is extremely deformed, the ALE algorithm is set as the explosive. The numerical model adopts the SOLID164 solid element and was modeled in proportion according to the design of the blasting scheme. To reduce the calculation workload, 11 support piles were selected for modeling, with a pile diameter of 1.8 m and a pile center distance of 1.5 m, and the crown beam structure was established at the top. The reserved rock mass is 8 m wide at the top and 10 m wide at the bottom, and the height difference from the blasting excavation surface is 8 m. The vibration-isolating slot is 4 m deep, 4 m wide at the top, and 3 m wide at the bottom. Because of the independent stress transfer process between the groups in the detonating network, a set of holes (the number of holes is 6) in the network was selected for modeling, and the parameters used are as follows: (i) the difference between the holes was set as 45 ms, (ii) the equivalent volume in the holes was set as no. 2 rock emulsion explosive of 6 kg, (iii) the hole spacing was 3.0 m, (iv) the row spacing was 2.5 m, and (v) the termination time was set as 450 ms. The relative position and mesh division of the model are shown in Figure 6.

4.1.2. Model Parameters. The model materials are pile and crown beam reinforced concrete materials, geotechnical materials, explosive materials, stemming materials, and air materials.

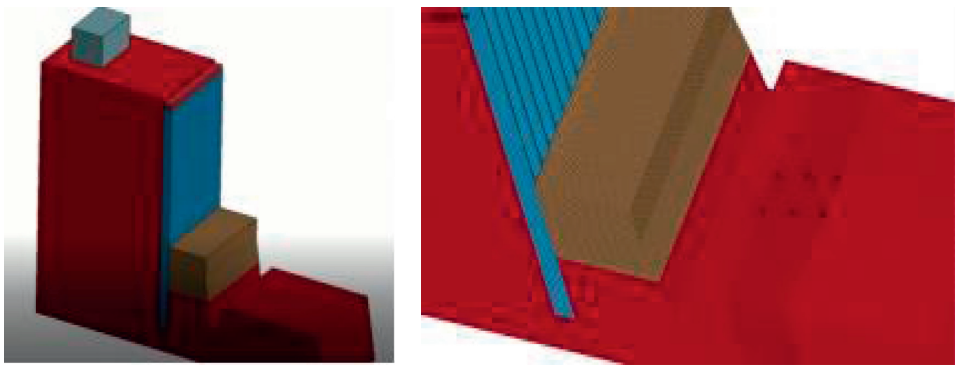

(a) (b)

Figure 6: Numerical calculation model: (a) the relative position and (b) mesh division.

(1) Reinforced Concrete Material Model. There are some difficulties in modeling the processing of reinforced concrete materials for supporting piles. To facilitate modeling and simplify the calculation, the equivalent modulus treatment method was selected for modeling of reinforced concrete materials by referring to relevant studies on elastoplasticity constitutive models of reinforced concrete [19, 20]; that is, according to the fraction of reinforcement in section and concrete strength, the reinforcement in reinforced concrete materials was dispersed among the materials for homogeneity.

According to relevant specifications, the concrete material is C30 with a Young's modulus of 30 GPa and a Poisson's ratio of 0.2, the fraction of reinforcement in the section is 2%, and Young's modulus of reinforcement is 200 GPa. During the modeling process, the *MAT_BRITTLE_DAMAGE_(TITLE) (096) model was selected, and relevant parameter settings are listed in Table 3.

(2) Geotechnical Material Model. The geotechnical material itself is nonhomogeneous and is also filled with structural planes such as joints and cracks. To simplify the calculation, it was idealized into homogeneous and continuous elastic-plastic materials in the simulation process. In this study, the *MAT_PLASTIC_KINEMATIC_(TITLE) material model was used to simulate the geotechnical material, and its mechanical parameters are listed in Table 4.

(3) Explosive Material Model. The no. 2 rock emulsion explosive was used in blasting construction, and the maximum single-hole charge in the simulation process is 6 kg. The *MAT_HIGH_EXPLOVE_BURN explosive material model with a mass density of 1200 kg/m was used. Its detonation velocity is 4500 m/s. The detailed parameters are shown in Table 5. According to the nature of rock mass and its stress state in the process of the explosion, the JWL equation of state was used to simulate the relationship between the pressure and specific volume in the process of explosive detonation, namely,

$$P = A\left(1 - \frac{\omega}{R_1 V}\right)e^{-R_1 V} + B\left(1 - \frac{\omega}{R_2 V}\right)e^{-R_2 V} + \frac{\omega E}{V}, \quad (1)$$

where A, B, R_1, R_2, and ω are the material constants; P is the pressure from the equation of state; V is the relative volume; E_0 is the internal energy density per unit initial volume.

(4) Stemming Material Model. The rock powder and mud from the drilling hole were used for on-site stemming. The material model of *MAT_SOIL_AND_FOAM was selected. The main parameters are shown in Table 6.

Because of the complexity of the building structure, the structure was no longer modeled separately to simplify the numerical calculation process, and the vibration velocity waveform of the bottom node near the foundation pit side of residential building (actual monitoring point of the project) was taken for analysis.

4.2. Verification of the Numerical Results. In the numerical modeling, referring to the actual engineering environment, the residential building on the north side of the adjacent foundation pit was taken as the research object, and the vibration waveform of the bottom node (the actual monitoring point) of the residential building near the foundation pit was verified.

The tested and the simulated vibration waveform are plotted in Figure 7, indicating that the trend of the curve for the tested and simulated vibration velocity versus time basically coincides, and the peak value of the simulated vibration velocity is 0.350 cm/s, while the tested peak value is 0.277 cm/s. The value of numerical simulation is high, and the relative error with the tested value is 20.8% because the modeling process idealizes the size structure of the vibration-isolating slot, geotechnical medium, surrounding topography, and explosive state equation. Although there is a certain difference between the simulated and the tested value, the numerical result data within the difference range are reasonable and feasible.

4.3. The Numerical Effect. According to the delay time of blasthole initiation, the von Mises stress cloud diagram after the blasting of no. 1, no. 3, no. 4, and no. 6 blastholes was taken, as shown in Figure 8, indicating that, in the blasting process of a single group of blastholes, as the number of

Table 3: Material parameters of the reinforced concrete.

Variable	Mass density (*RO*)	Young's modulus (*E*)	Poisson's ratio (*PR*)	Tensile limit (*TLIMIT*)	Shear limit (*SLIMMIT*)	Fraction of reinforcement in section (*FRA RF*)	Young's modulus of reinforcement (*ERF*)
Units	kg/m³	GPa	—	GPa	GPa	—	GPa
Value	2500	30	0.2	$4.02E-3$	$2.1E-2$	0.02	200

Table 4: Rock material parameters.

Variable	Mass density (RO)	Young's modulus (*E*)	Poisson's ratio (PR)	Yield stress (SIGY)
Units	kg/m³	GPa	—	GPa
Value	2430	48.3	0.26	$3.0E-2$

Table 5: Related parameters of the state equation of detonation products.

Variable	Mass density (RO)	Detonation velocity (*D*)	The material constants					The internal energy density per unit initial volume (E_0)
			A	*B*	*R1*	*R2*	ω	
Units	$\mathrm{Kg \cdot m^{-3}}$	$\mathrm{m \cdot s^{-1}}$	GPa	GPa	—	—	—	GPa
Value	1200	4500	255	5.58	5.66	1.49	0.37	9.14

Table 6: Parameters of stemming material.

Variable	Mass density (RO)	Bulk modulus (*K*)	Shear modulus (*G*)	Yield function constant			Pressure cutoff (PC)
				(*A*0)	(*A*1)	(*A*2)	
Units	g/cm³	GPa	GPa	—	—	—	—
Value	1.80	$6.3E-4$	0.3	$3.4E-13$	$7.0E-7$	$-6.9E-8$	0

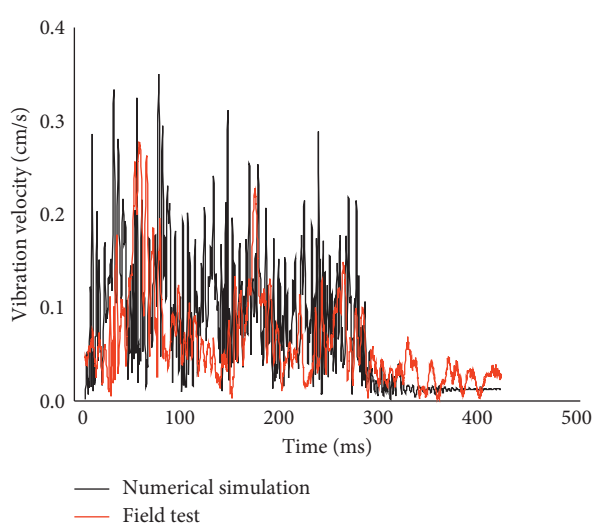

Figure 7: Combined vibration waveform.

blastholes increases, the stress concentration range in the blasting area increases, and the stress concentration in the blasting area gradually increases, reflecting the rock-breaking process to a certain extent.

According to the stress nephogram, the rock mass in the left side of the vibration-isolating slot is basically blue with small stress, indicating that the slot plays a blocking role in the transfer of blasting stress and effectively protects the foundation pit supporting system and existing buildings on the left side of the slot. To quantify the barrier effect of the vibration-isolating slot on the blasting stress, the stress versus time curve of the characteristic points 10 m from the center of the detonation zone to the direction of the vibration-isolating slot and the opposite direction was taken, as shown in Figure 9. The peak stress of the characteristic points on the side without the vibration-isolating slot and that on the side with the slot were extracted, and the corresponding peak stress was found as 8.45 and 1.48 MPa, respectively. The peak stress of the characteristic points on the side of the vibration-isolating slot was only 17.6% of that on the other side, proving that the vibration-isolating slot is an economical and efficient engineering measure for the protection of the structure near the area.

4.4. Dynamic Response Characteristic Analysis. The most unfavorable factor of blasting excavation for the foundation pit is the disturbance caused by blasting stress to the supporting structure. The safety and stability of the structure depend on its dynamic response under blasting disturbance. Therefore, the dynamic response law of displacement, stress, strain, and velocity was investigated to provide reference for vibration control and prediction. The response characteristics of displacement, velocity, stress, and strain of the supporting pile were studied starting from the center of the top of the pile and taking the nodes and corresponding units of the supporting pile axis vertically downward every 10 m. The node numbers are 846585, 848037, 848169, 849554, and

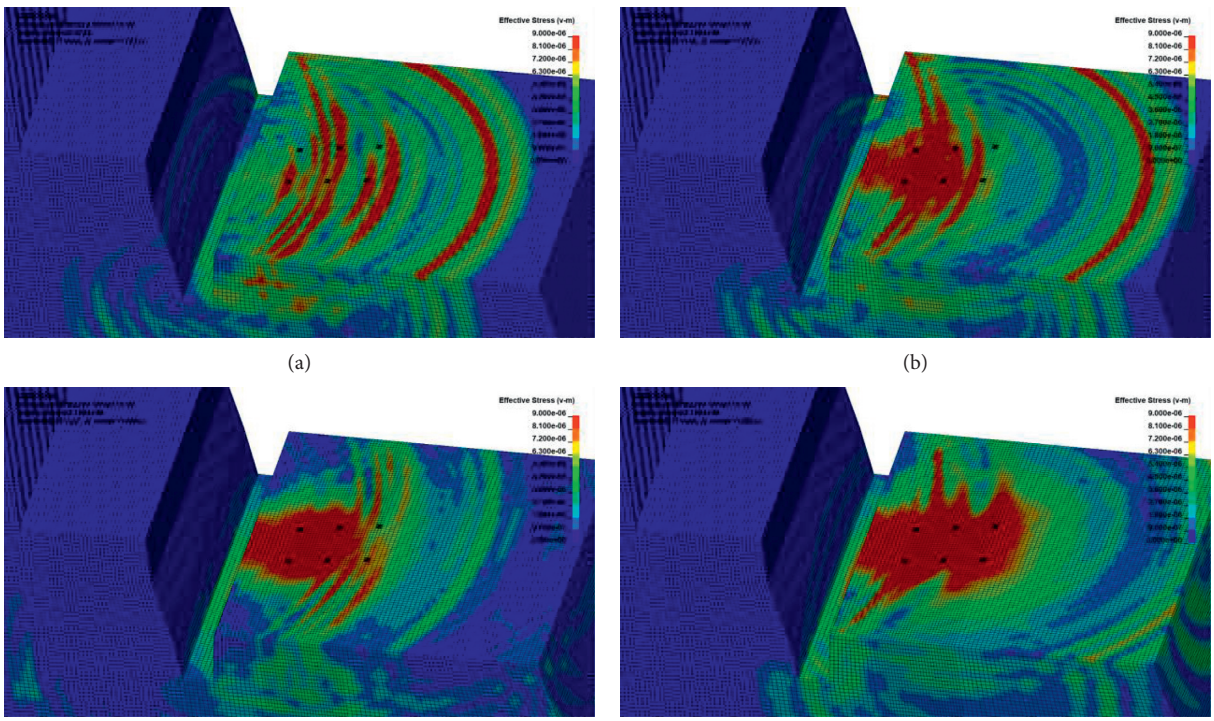

Figure 8: Stress nephogram of blasthole blasting: (a) no. 1 blasthole ($t = 30$ ms), (b) no. 3 blasthole ($t = 120$ ms), (c) no. 4 blasthole ($t = 150$ ms), and (d) no. 6 blasthole ($t = 240$ ms).

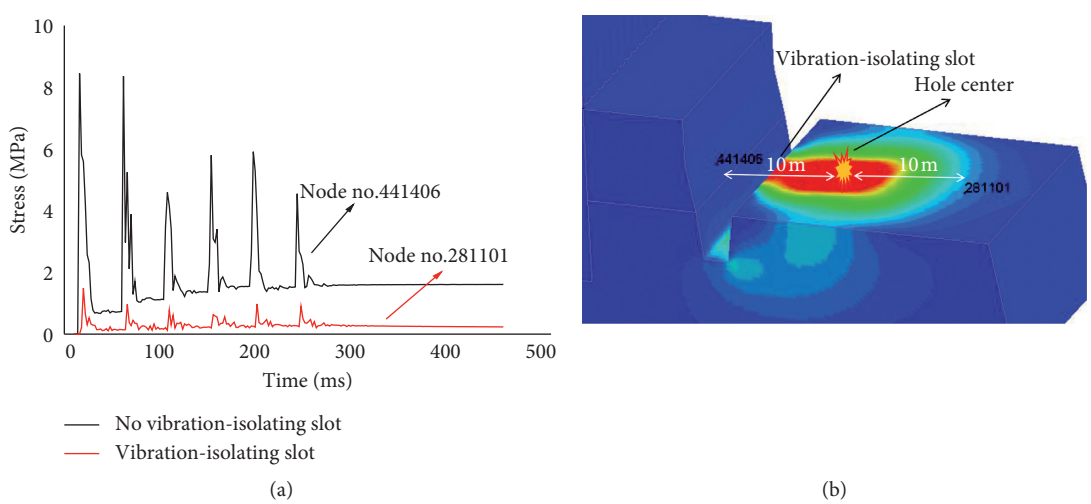

Figure 9: Stress comparison of characteristic points. (a) Stress vs. time curve; (b) the position of characteristic points.

849915, and the unit numbers are H1545060, H1545492, H1546434, H1546467, and H1547250, as shown in Figure 10.

4.4.1. Displacement Response Characteristics of the Supporting Pile. Figure 11 shows the displacement versus time response curves of the nodes at different positions of the supporting pile axis.

Figure 11 shows that the displacement of the axial node of the supporting pile is large in the X direction, followed by in the Y direction, and smallest in the Z direction and is related to the position applied by blasting stress. The overall displacement of the node reflects the movement of the pile. When the displacement is about 300 ms, the node itself shows reciprocating movement, and the displacement does not change dramatically during the reciprocating process. The node in the numerical calculation process did not show any failure, indicating that there is no damage inside the pile body under the stress disturbance.

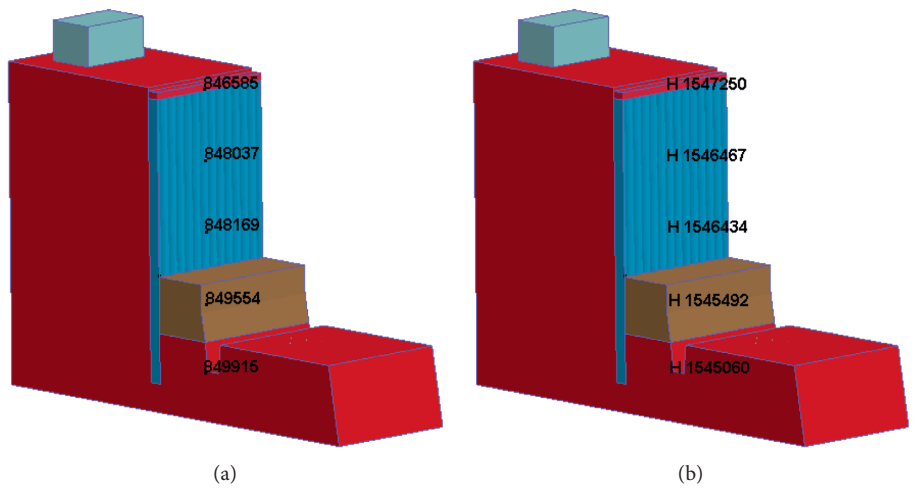

Figure 10: Axis characteristic points of the supporting pile: (a) nodes; (b) the units corresponding to the nodes.

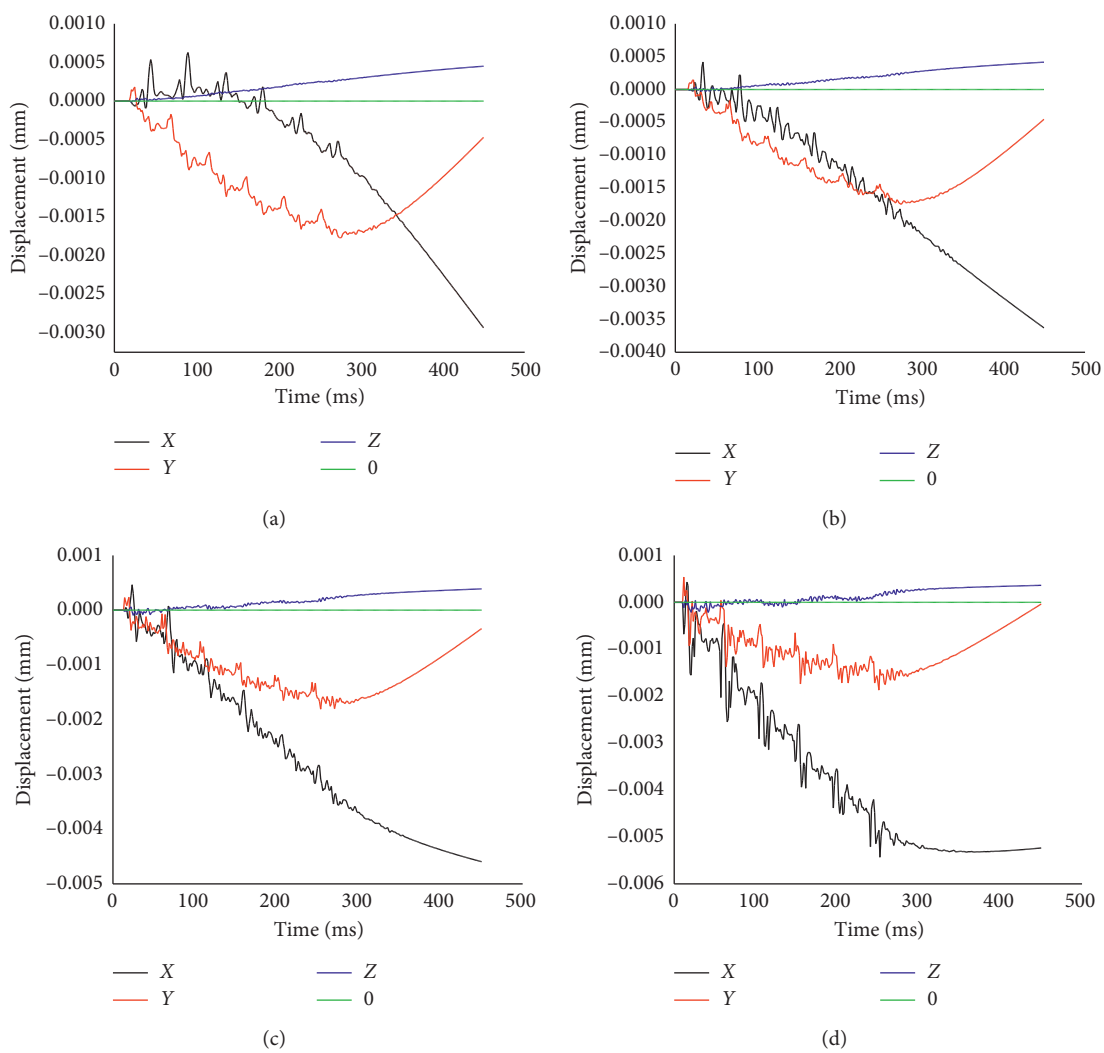

Figure 11: Continued.

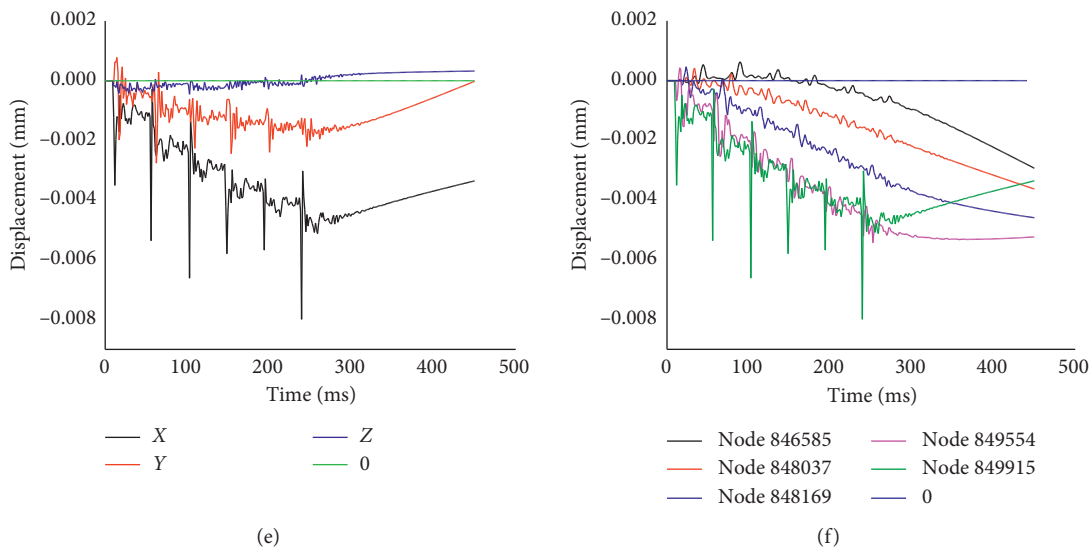

Figure 11: The displacement versus time response curves for the supporting pile: (a) node no. 846585, (b) node no. 848037, (c) node no. 848169, (d) node no. 849554, (e) node no. 849915, and (f) the X direction.

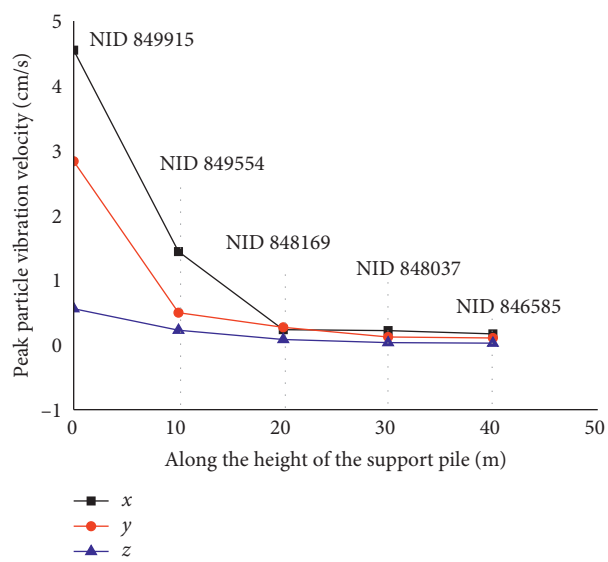

Figure 12: The response trend of PPV in three directions with increasing supporting pile height.

In the calculated step size, the displacement of no. 849915 node, which is closest to the explosion zone, is the maximum, reaching 0.081 mm in the X direction. The displacement of the bottom three characteristic points (node no. 849915, no. 849554, and no. 848169) in the X direction showed a recovery trend. Each node displacement in the X direction versus time response curves is shown in Figure 11(f). The bottom node of the supporting pile moves directly in the negative X direction after being disturbed by the blasting stress, while the top node first moves slightly in the positive X direction and then moves in the negative X direction. This reflects the movement process of the rod body after being stressed and is following the motion law of the elastic rod body.

4.4.2. Velocity Response Characteristics of the Supporting Pile. The response trend of vertical, horizontal radial, and tangential PPV with increasing supporting pile height under the action of the electronic detonator initiation and the vibration-isolating slot is statistically shown in Figure 12, indicating that the PPV is radial $X >$ tangential $Y >$ vertical Z and is consistent with the experimental outcome. At the bottom of the pile, the radial, tangential, and vertical PPVs are the largest, with 4.55, 2.83, and 0.56 cm/s, respectively, whereas at the top, they are small with the values of 0.17, 0.11, and 0.03 cm/s, respectively. The PPV of the blasting response in each direction attenuates strictly with increasing supporting pile height, and there is no "elevation amplification effect." It can be considered that the existence of the vibration-

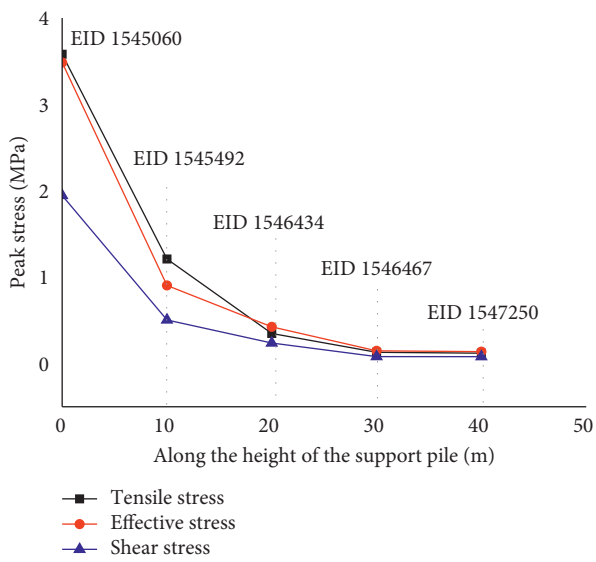

Figure 13: The response trend of the peak stress with the increase in the supporting pile height.

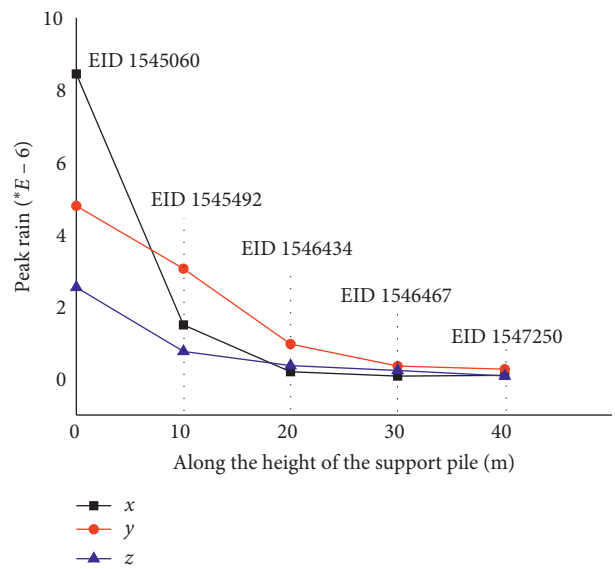

Figure 14: The response trend of the peak strain with the increase in the supporting pile height.

isolating slot has an obvious effect on seismic wave propagation. The radial and the tangential peak vibration velocity attenuate sharply along with the pile in the range of 0–20 m. The inflection point appears at 20 m, and the attenuation tends to be gentle in the range of 20–40 m. The vertical PPV is flat with increasing pile height and is generally gentle.

4.4.3. Stress Response Characteristics of the Supporting Pile. Figure 13 shows the response trend of tensile stress, effective stress, and shear stress with increasing supporting pile height under the action of the electronic detonator initiation and the vibration-isolating slot. Clearly, the variation trend of tensile stress, effective stress, and shear stress peak is consistent and decreases with increasing pile height, and the peak stress at the bottom of the pile reaches the maximum value of 3.58, 3.48, and 1.95 MPa, respectively, and the peak stress is the smallest at the top with 0.12 MPa, 0.14 MPa, and 0.08 MPa, respectively. According to the strength theory, all the stresses are less than 4 MPa and the supporting piles are in a safe state. The height along the pile is in the range of 0–20 m in the following order: peak tensile stress > effective stress > shear stress. The height along the pile is in the range of 20–40 m, in the following order: peak effective stress > tensile stress > shear stress.

4.4.4. Strain Response Characteristics of the Supporting Pile. Figure 14 shows the strain response trend of vertical, horizontal radial, and tangential directions with increasing supporting pile height under the action of the electronic detonator initiation and the vibration-isolating slot, indicating that the variation trend of the vertical, tangential, and radial strain peaks is consistent, and they all decrease with increasing pile height. The maximum strain peaks at the bottom of the pile are 2.5, 4.8, and 8.4, respectively, and at the top is the smallest, at 0.08, 0.3, and 0.1, respectively. The height along the pile is in the range of 0–20 m, and the strain follows the order horizontal > vertical. The height along the pile is in the range of 20–40 m with the strain value in the following order: tangential > vertical > radial.

5. Conclusion

Based on the ultradeep foundation pit excavation in the complex environment around Liuguangmen, Guiyang city, an effective blasting model of vibration-isolating slot and electronic detonator was successfully established, the vibration response characteristic test and dynamic response numerical test were carried out, and the dynamic response characteristics of existing structures under the blasting action of 6 kg single-hole charge were studied. The outcome of this study is as follows:

(1) The vibration velocity and stress of the structure are in a safe range under the action of excavation vibration-isolating slot and electronic detonator initiation. In addition, the efficient blasting excavation scheme was found to be feasible, ensuring the safety of the surrounding existing buildings.

(2) The detonation of the electronic detonator carries out peak shaving within the group, unloading waves between the groups, and the blocking effect of the vibration-isolating slot, effectively reducing the peak stress and PPV, evenly distributing the vibration velocity, and ensuring the safety and efficiency of ultradeep foundation pit excavation in the complex urban environment. There is a contact surface between the supporting pile and the rock mass, and the stress wave in the surface is reflected and stretched, resulting in the "wall effect", and the propagation velocity is lower than that inside the rock mass. The PPV is in the following order: radial X > tangential Y > vertical Z.

(3) Under the action of the electronic detonator initiation and vibration-isolating slot, the peak values of stress, strain, and PPV all show a decreasing trend with increasing supporting pile height, and there is an inflection point at 20 m. In the 0–20 m range, the peak stress is tensile > effective > shear, the peak strain is horizontal > vertical, and the PPV attenuates rapidly. In 20–40 m range, the peak stress value is effective > tensile > shear, the peak strain value is in the order tangential > vertical > radial, and the PPV attenuates gently.

(4) The internal nodes of the pile reciprocate without sharp change and failure in displacement. The peak displacement of different nodes with increasing pile height is in the following order: $X > Y > Z$. The maximum displacement value of the axial node of the pile within the calculated step size (45 ms) is 0.08 mm, which is located at the bottom of the pile, and its motion direction is opposite to the explosion zone with a trend of recovery, while the displacement is located at the top of the pile and its motion direction is first toward the explosion zone and then the reverse zone, following the motion law of the elastic rod body.

Data Availability

The data used to support the findings of this study are available from the corresponding author upon request.

Conflicts of Interest

The authors declare no conflicts of interest.

Acknowledgments

This study was supported by the National Natural Science Foundation of China (Grant no. 51664007).

References

[1] Y. J. Li, W. Zhao, G. R. Zhao et al., "Controlled blasting evacuation technique for ultra-deep foundation pits in downtown area," *Engineering Blasting*, vol. 25, no. 5, pp. 42–45, 2019.

[2] T. Gao, C. B. Zhou, N. Jiang et al., "Study on the vibration velocity threshold of the adjacent pipeline under the blasting excavation of the foundation pit," *Journal of Safety and Environment*, vol. 17, no. 6, pp. 2191–2195, 2017.

[3] X. N. Ma, S. X. Zhao, and X. Ai, "Shaking table test study on deep pit supporting," *Journal of Lanzhou Jiaotong University*, vol. 34, no. 1, pp. 1–5, 2015.

[4] X. D. Zhang, C. G. Zhang, and J. S. Liu, "Analysis on stability of deep foundation pit supporting structure under traffic loads," *The Chinese Journal of Geological Hazard and Control*, vol. 22, no. 2, pp. 125–129, 2011.

[5] X. M. Zhang, Y. F. Shi, Z. L. Zhang et al., "Dynamic response of enclosure structure of an unsymmetrical loaded foundation pit under train induced dynamic load," *Journal of Vibration and Shock*, vol. 31, no. 20, pp. 103–109, 2012.

[6] B. Xie, H. B. Li, Y. Q. Liu, and X Xia, "Study of safety control of foundation pit excavation by blasting in ningde nuclear power plant," *Chinese Journal of Rock Mechanics and Engineering*, vol. 28, no. 8, pp. 1571–1578, 2009.

[7] C. H. Dowding, E. Hamdi, and C. T. Aimone-Martin, "Strains induced in urban structures by ultra-high frequency blasting rock motions: a case study," *Rock Mechanics and Rock Engineering*, vol. 49, no. 10, pp. 4073–4090, 2016.

[8] D. Z. Yankelevsky, S. Schwarz, and B. Brosh, "Full scale field blast tests on reinforced concrete residential buildings—from theory to practice," *International Journal of Protective Structures*, vol. 4, no. 4, pp. 565–590, 2013.

[9] B. Meins, C. Aimone-Martin, C. Woznick et al., "Tall structure response to close-in urban blasting in New York city—part 2," *Journal of Explosives Engineering*, vol. 32, no. 6, pp. 6–15, 2014.

[10] X.-B. Xie, X.-Z. Wang, and Q.-C. Tang, "Urban shallow-buried tunnel driving blasting in complicated enviroment," *Blasting*, vol. 31, no. 3, pp. 91–95, 2014.

[11] D.-B. Wang, M. A. Hong-Hao, Z.-W. Shen et al., "Blasting vibration damping and monitoring of foundation pit under urban complex environment," *Engineering Blasting*, vol. 21, no. 1, pp. 47–51, 2015.

[12] Q. Zhou, H. G. He, S. F. Liu et al., "Blast resistance evaluation of urban utility tunnel reinforced with BFRP bars," *Defence Technology*, 2020, In press.

[13] Y. Q. Zhang, N. Jiang, C. B. Zhou et al., "Dynamic response of building structures with high-rise frames caused by blasting vibration at adjacent subway foundation pit," *Journal of China Coal Society*, vol. 44, no. s1, pp. 118–125, 2019.

[14] Y. Y. Wang, L. J. Gu, X. C. Huang et al., "Destruction process numerical simulation of underground pit supporting system under earthquake action," *Journal of Shanghai Jiaotong University*, vol. 45, no. 5, pp. 767–771, 2011.

[15] L. W. Wei, B. Zhang, F. L. Han, and X. Zhang, "Damping and blasting technology for 45 m deep foundation pit," *Journal of Chongqing Jiaotong University (Naturnal Science)*, vol. 33, no. 3, pp. 38–40, 2014.

[16] C. Y. Sun, L. Xue, S. B. Liu et al., "Experimental and numerical simulation on vibration reduction effect of damping holes for deep foundation pits," *Acta Armamentarii*, vol. 38, no. s1, pp. 237–242, 2017.

[17] State Administration of Work Safety, *Safety Regulations for Blasting: GB 6722-2014*, China Standards Press, Beijing, China, 2015.

[18] Y. Y. Wang, L. J. Gu, X. C. Huang et al., "Stability analysis of foundation pit support system on earthquake action," *Journal of Shanghai Jiaotong University*, vol. 45, pp. 21–26, 2011.

[19] X. P. Shen, C. Y. Wang, and L. Zhou, "A plastic constitutive model for reinforced concrete damage and its engineering application," *Engineering Mechanics*, vol. 24, no. 6, pp. 122–128, 2007.

[20] D. D. Kong, Y. H. Zhao, P. Wang et al., "Equivalent modulus method in finite element analysis of reinforced concrete materials," *Journal of Shenyang Jianzhu University (Natural Science Edition)*, vol. 21, no. 3, pp. 122–128, 2005.